SILICON PROCESS- NEW HOOD DESIGN FOR TAPPING GAS COLLECTION

M. Kadkhodabeigi[1], H. Tveit[2] and K. H. Berget[3]

[1] Department of Materials Science and Engineering, Norwegian University of Science and Technology (NTNU), PO Box 7491, Trondheim, Norway; mehdi.kadkhodabeigi@material.ntnu.no
[2] Elkem Thamshavn, PO Box 10, N-7301, Orkanger, Norway; halvard.tveit@elkem.no
[3] Elkem Silicon Materials, PO Box 5211, Majorstuen 0303, Oslo, Norway; kjell.hakon.berget@elkem.no

ABSTRACT

Gassing from the taphole of submerged arc furnaces used for silicon production poses a significant problem in the view of environment, operation and economy of production. The reason for the gassing is the pressure of the process gasses in the furnace (mainly CO and SiO) which may escape through the taphole. The combustion of the off gasses creates a high temperature gas containing very fine particles of SiO_2 and the result may be internal pollution in the tapping area. This study presents development of a model for combustion and capturing of the off gasses from the furnace taphole as the preliminary design of a new hood system for Elkem Company. The developed model is 3D and is constructed based on CFD method as a powerful tool to reach the desired results. In this paper several case studies consist of different velocities and components for the off gasses and different suction rates for the fans have been considered. The results show that based on the designed geometry and selection of the right suction rate for the fan it is possible to capture the off gasses from the taphole and to reduce the air pollution problems in the tapping area. Experimental observations and measurements after installing the new hood design over the taphole of the furnace validate the results of the model.

1 INTRODUCTION

Tapping of the molten metal from the furnace heart has always been a big challenge in the silicon production process. In the tapping process a flow of silicon melt with temperatures around 1600°C has to be controlled. Therefore the tapping area includes some potentially hazardous working conditions [1]. One of the key issues which affect the tapping process in aspects of safety, environment and economy of production is taphole gassing phenomena. The taphole gassing phenomena usually happens when the furnace taphole is opened to remove the accumulated melt at the furnace bottom. The phenomenon includes blowing-out of high velocity and high temperature jet of a gas from the taphole. The gas is composed of SiO and CO which due to its high temperature reacts with oxygen in the air and produces fine SiO_2 particles and a gas rich of CO_2 [2].

Existence of high pressure gas in the crater zone of the furnace creates the potential for the process gas to be removed from taphole while tapping silicon melt from the furnace. If the taphole channel is well defined and filled with silicon metal, no gas will penetrate through the taphole. But if the taphole, especially the inner part is uneven and consists of several “trumpet”-shaped channels, there may be free flow of gas from the crater to the taphole opening. Normally, there will be a low internal flow resistance from the crater to the inner opening of the taphole channel. Figure 1 shows a schematic of the furnace inside and taphole gassing phenomena.

Finding a solution for capturing the off-gasses from the taphole has several advantages such as reduction of internal pollution in the plant, making more safe working conditions for the operators in the tapping area and recovery of fine SiO_2 particles which has economic benefits.

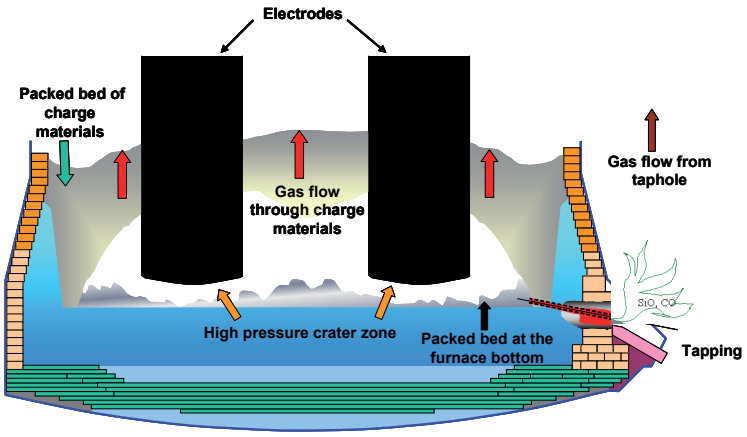

Figure 1: Schematic of furnace inside and the taphole gassing phenomena [1].

In this paper a 3D computational fluid dynamics (CFD) model of the taphloe gassing phenomena in the silicon production furnaces is presented. The aim of this research was to investigate the feasibility of constructing a capturing system for off-gasses from the furnace taphole during the gassing phenomena. Most furnaces are equipped with an off-gas system in order to take care of taphole gasses in the normal situation. The ideas introduced in this work, through designing the new hood system, is to take care of more sever gassing situations. The new hood design is a suction system which is installed over the taphole to direct the blowing gasses from taphole towards the main off-gas channel at the furnace top.

In order to be able to study different gassing conditions, several case studies have been investigated by the model. A wide range of velocities for the off-gasses from the taphole together with different suction rates for the new hood design fan was investigated. The combustion of high temperature SiO and CO gasses as the result of chemical reaction with oxygen in the air and the resulted flame was modeled. The composition of the off-gas which is a mixture of SiO and CO determines the temperature distribution due to combustion.

The results of experimental tests at Elkem Thamshavn plant, where the new hood design has been installed, were in good agreements with the results of the CFD model and hence it shows the validity of the model.

2 TAPHOLE GASSING PHENOMENA

2.1 Root Reasons for Taphole Gassing

The reactions in the silicon production furnace can be formally treated as a combination of gross two reactions, equations (1) and (2).

$$SiO_2(s,l) + 2C(s) = Si(l) + 2CO(g) \quad (1)$$

$$SiO_2(s,l) + C(s) = SiO(g) + CO(g) \quad (2)$$

The quartz and the carbon are added in a condensed state, and the products are mainly in a gaseous phase as CO and SiO. Also according to the gas law, the high temperature in the reaction zone will increase the volume of the gas. In a silicon furnace of 24 MW, the amount of added material is in the order of 1 liter per second. The volume of the CO gas and the SiO gas produced in the crater will be in the order of 10 m^3 gas per second [1]. This huge production of process gas in the crater zone and the resistance against gas flow in the charge materials, results in a higher pressure in the crater zone than outside the furnace.

The extent of chemical reactions (1) and (2) is directly connected to the furnace electric load. Therefore electric load change can affect the level of chemical reactions. Previous studies about the gas pressure in the crater zone of the silicon furnace shows a direct relation between electric load and crater pressure [1]. This relation is presented in Figure 2.

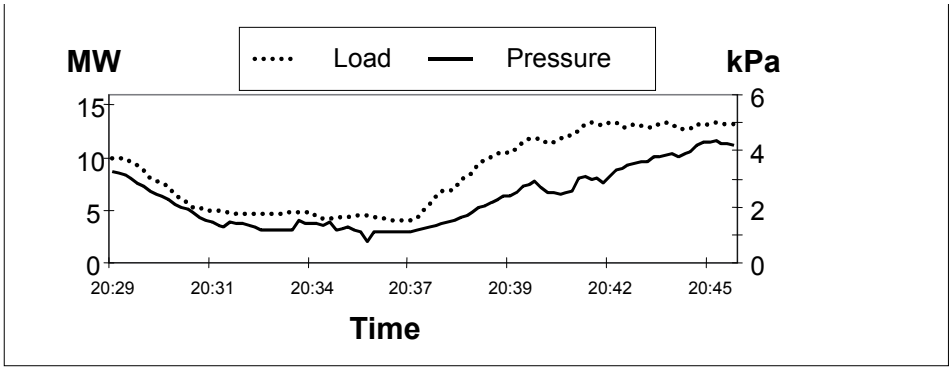

Figure 2: Measured crater pressure and electrode load at Elkem Thamshavn [1].

High pressure gas in the crater zone flows towards furnace top through passing the charge materials. Different chemical reactions between process gas and charge materials happen in different regions of the furnace [2]. Condensation of SiO gas in the upper part of charge materials happens through the following reaction:

$$2SiO(g) = Si(l) + SiO_2(s,l) \quad (3)$$

Condensation of SiO gas according to reaction (3) causes the charge materials in the upper part of the furnace glue together and therefore porosity of charge materials in that region decreases. Lower permeability of charge materials will lead to higher resistance against gas flow. Therefore this phenomena itself helps the formation of higher gas pressure in the crater zone of the furnace.

As it can be seen there are different reasons for high gas pressure inside the furnace. Combination of the above mentioned reasons for existence of a high pressure crater zone together with other operational issues related to tapping of silicon melt, will lead to happening of taphole gassing phenomena.

2.2 Different Aspects of Taphole Gassing

As a result of direct contact between the off-gasses from the taphole and the oxygen in the air the rapid combustion of SiO and CO gas occurs according to the following reactions:

$$SiO(g) + 1/2O_2(g) = SiO_2(s) \quad (4)$$

$$CO(g) + 1/2O_2(g) = CO_2(g) \quad (5)$$

Produced SiO_2 is in the form of very fine particles and CO_2 is also in the form of a high temperature gas. Therefore the taphole gassing phenomena is known as an important internal source of pollution in the silicon production plant.

The gassing is stated suddenly after the taphole is opened and in severe cases the length of the blowing jet of hot gas can reach up to few meters. Therefore it can create a dangerous condition for the operators who are working in the tapping area. Previous studies have reported several accident and human damages due to taphole gassing [1].

The main outlet for the process gas is through the charge materials, where it is collected in the furnace hood and sent to the filter. SiO gas is an intermediate product in the silicon furnace and it is recovered through reaction with the charge materials in the furnace before escaping from the furnace top. During the gassing phenomena the SiO gas will find its way out of furnace through taphole. Therefore the taphole gassing affects the economy of the silicon production as well.

3 NEW HOOD DESIGN AND ITS STRUCTURE

In order to capture the off-gas from furnace taphole during tapping process, development of a new hood design is necessary. The new hood design is in fact a suction system which is installed over the

furnace taphole. The new hood design is like a channel which has an inlet is over the taphole and the outlet which is connected to the main ventilation system of the furnace, which itself contains a very big and high capacity intake fan. Figure 3 shows schematic view of the new hood design and the related structure.

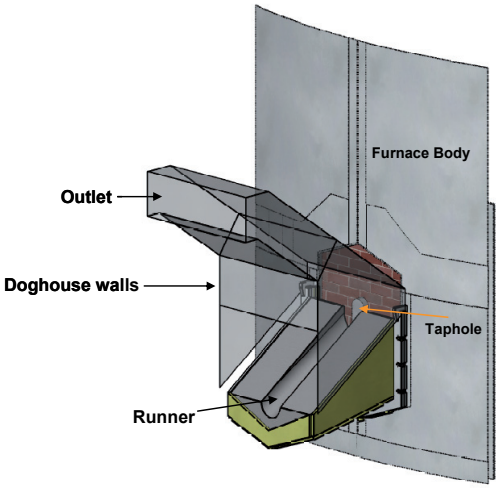

Figure 3: Schematic of the structure of the new hood design.

As it can be seen from Figure 3 the structure of the new hood system has been designed so that it will not create any problem for the operators during opening and closing of the taphole. In the other hand if there is enough suction rate at the outlet it is possible to capture large portion of the fumes leaving the ladle under runner.

4 MATHEMATICAL MODELING

4.1 Description of CFD Model

In order to investigate the capability of the new ventilation system for taphole off-gas a CFD model of the structure of the new hood design was developed. The model is 3D and contains all aspects of the problem such as gas blowing out, air flow around the taphole, chemical reactions due to combustion of off-gasses, different heat transfer mechanisms and temperature distribution in different parts of the system. The geometries in the model were selected based on the proposed industrial design by Elkem Company.

4.1.1 Transport equations

The equations which are solved in the CFD model are the continuity, momentum and energy equations. These equations are presented as the following general transport equation [3].

$$\frac{\partial}{\partial t}(\rho\phi)+\nabla\cdot\left(\rho\phi u-\alpha\Gamma_{\phi}\nabla\phi\right)=S_{\phi} \tag{6}$$

Where φ represents the variables solved in the model such as mass, velocity and energy, ρ is the density of fluid, Γ_{φ} is the effective diffusion coefficient and S_{φ} is the source term.

4.1.2 Species equation

$$\frac{\partial}{\partial t}(\rho Y_i)+\nabla\cdot\left(\rho\vec{v}Y_i\right)=-\nabla\cdot\vec{J}_i+R_i+S_i \tag{7}$$

In which the diffusion flux of species *i* for turbulent flows, can be written as [4]:

$$\vec{J}_i = -\left(\rho D_{i,m} + \frac{\mu_t}{Sc_t}\right)\nabla Y_i \tag{8}$$

Where Y_i is mass fraction of species i, $D_{i,m}$ is diffusion coefficient for species i, μ_i is turbulent viscosity and Sc_i is the Schmidt number.

The species equation describes that the rate of change of the mass of the chemical species per unit volume is equal to the rate of generation of the chemical species minus the convection and diffusion fluxes per unit volume. The first left hand term represents the rate of increase of species *i* into the fluid element; the second term the net rate of flow of species *i* out of the fluid element due to convection. On the right hand side the first term describes the rate of increase of species *i* due to diffusion. R_i is the net rate of production of species *i* by chemical reaction and S_i is the rate of creation by addition from the dispersed phase plus any user defined sources.

4.1.3 Turbulent model

Due to turbulent nature of the process under consideration, the standard *k-ε* turbulent model was used in this work. The standard *k- ε* is a semi-empirical model based on model transport equations for the turbulence kinetic energy (*k*) and its dissipation rate (*ε*). The transport equations for turbulence kinetic energy and its dissipation rate can be obtained from the Navier-Stokes equations by a sequence of algebraic manipulations. The two equations for *k* and *ε* can be expressed as follows [5]:

$$\frac{\partial}{\partial t}(\rho k) + \frac{\partial}{\partial x_i}(\rho k u_i) = \frac{\partial}{\partial x_j}\left[\left(\mu + \frac{\mu_t}{\sigma_k}\right)\frac{\partial k}{\partial x_j}\right] + G_k + G_b - \rho\varepsilon - Y_M + S_k \tag{9}$$

$$\frac{\partial}{\partial t}(\rho \varepsilon) + \frac{\partial}{\partial x_i}(\rho \varepsilon u_i) = \frac{\partial}{\partial x_j}\left[\left(\mu + \frac{\mu_t}{\sigma_\varepsilon}\right)\frac{\partial \varepsilon}{\partial x_j}\right] + C_{1\varepsilon}\frac{\varepsilon}{k}(G_k + C_{3\varepsilon}G_b) - C_{2\varepsilon}\rho\frac{\varepsilon^2}{k} + S_\varepsilon \tag{10}$$

G_k represents the generation of turbulence kinetic energy due to the mean velocity gradients and G_b is the generation of turbulence energy due to buoyancy. Y_M represents the contribution of the fluctuating dilatation in compressible turbulence to the overall dissipation rate while $C_{1\varepsilon}$, $C_{2\varepsilon}$ and $C_{3\varepsilon}$ are constants. σ_ε and σ_k are the turbulent Prandtl numbers for *k* and *ε* respectively. S_k and S_ε are source terms. The empirical parameters used in this model are listed in Table 1.

Table 1: Model constants used in the *k-ε* model

C_μ	σ_k	σ_ε	$C_{1\varepsilon}$	$C_{2\varepsilon}$
0.09	1.0	1.3	1.44	1.92

4.1.4 Radiation model

The gas radiation in this study is modeled by using the standard P1 model. The P1 radiation model is based on the expansion of the radiation intensity into orthogonal series of spherical harmonics. The radiative flux is given by equation (11) where *G* is the incident radiation and *C* is the linear-anisotropic phase function coefficient [6, 7].

$$q_r = -\Gamma\nabla G \tag{11}$$

$$\Gamma = \frac{1}{(3(a+\sigma_S) - C\sigma_S)} \tag{12}$$

The transport equation for *G* is defined in equation (13) where *σ* is the Stefan-Boltzmann constant and S_G is a user-defined radiation source.

$$\nabla\cdot(\Gamma\nabla G) - aG + 4a\sigma T^4 = S_G \tag{13}$$

Equation (13) is solved in order to determine the local radiation intensity. Combining equations (11) and (13) gives lead to Equation (14) which can then be directly substituted into the energy equation to account for heat sources (or sinks) due to radiation.

$$\Delta q_r = aG + 4a\sigma T^4 \tag{14}$$

4.1.5 Combustion model

The combustion of off-gasses from taphole according to equations (4) and (5), affects the energy distribution and the velocity pattern of the gas flows in the system and must be taken into consideration in the modeling process. In the calculations related to combustion, the Eddy-Dissipation model was used. The reason to choose this approach is related to the turbulent nature of the gas flows.

Adiabatic temperature of combustion for both SiO and CO gas with oxygen in the air was calculated separately and the results were used in the model. In the calculations two assumptions were considered. First of all the combustion considered to be adiabatic and at constant volume and second of all perfect mixing of reactants with a mixing rate equal to 1 was applied. Table 2 shows the results of calculation of adiabatic temperature of combustion for some species. The density of gas mixture is calculated based on the mixture composition and gas temperature.

Table 2: Thermodynamic data for adiabatic temperature of combustion of some species.

Species	Enthalpy of formation (kJ/mol)	Specific heat (J/kg.K)
N_2	0	$939.8 + 0.2802T - 5.308\times10^{-5}T^2$
O_2	0	$854.1 + 0.2765T - 5.404\times10^{-5}T^2$
SiO	-98.4	$1.34 + 1.76\times10^{-4}T$
SiO_2	-910	$2.8 + 5.35\times10^{-4}T$
CO	-110	$940 + 0.3017T - 6.091\times10^{-5}T^2$
CO_2	-393.5	$581.4 + 1.089T - 5.215\times10^{-4}T^2 + 8.682\times10^{-8}T^3$

4.1.6 Boundary conditions

In order to perform calculations of CFD model different boundary conditions were defined. Definition of the boundary condition was done based on the structure of the ventilation system. According to the defined boundary conditions taphole was modeled as mass flow inlet. Because mixture of off-gasses is blown-out of the taphole during gassing phenomena. The outlet of the new hood design was modeled as outflow. The suction rate by the intake fan determines the amount of the off-gasses which flows through the outlet. The environment around the new hood design is modeled as atmospheric pressure inlet. Therefore the model is able to consider the effect of “Hall-Wind”. The part of runner walls which molten silicon flows through that into the ladle, were modeled as high temperature zone. The wall temperature considered to be around 1500°*C*. The reason to define high temperature boundary condition for this wall was to take into account the effect of metal flow on radiative heat transfer.

4.2 Geometry of the system

The taphole diameter was selected to be 7.5 *cm*. The real diameter in the silicon furnaces is more but during the gassing phenomena the off-gas does not blow-out from the total surface of the taphole. Because even in the taphole gassing mode there is some flow of metal from the taphole. Therefore the considered taphole diameter seems to be reasonable. Due to confidential reasons we are not allowed to give detailed geometrical design of the new hood system. However the height of the new hood design from the taphole level is around 2.5*m* and its width is around 1.2*m.*

Figures 4 and 5 represent the geometry used in the CFD model. In order to consider the effect of environment air flows on the performance of the system and therefore make the CFD model more

realistic, the area under consideration for modeling was extended to the space around the new hood design which contains atmospheric air flows.

4.3 Numerical Method

The numerical approach used in this study is based on finite volume method (FVM). In order to perform the simulations the commercial CFD software Fluent version 6.3.21 was applied. The transport equations for mass, momentum and energy together with prescribed different equations of heat transfer, combustion and turbulent flows are solved simultaneously.

Several simulations by defining of different gas velocities blown-out of the taphole and different suction rates by the furnace intake fan have been performed in this research. The reason for that is to consider different modes of the gassing phenomena from less intensive to most sever cases which may happen in real operation of the furnace. Different case studies are briefly presented in Table 2.

Table 3: List of different case studies (V is the taphole gas velocity and S is the suction rate of intake fan)

Case Studies	S=0 (Nm^3/hr)	S=5000 (Nm^3/hr)	S=15000 (Nm^3/hr)	S=30000 (Nm^3/hr)	S=60000 (Nm^3/hr)
V=10 m/s	√	√	√	√	
V=50 m/s	√	√	√	√	√
V=100 m/s	√	√	√	√	√

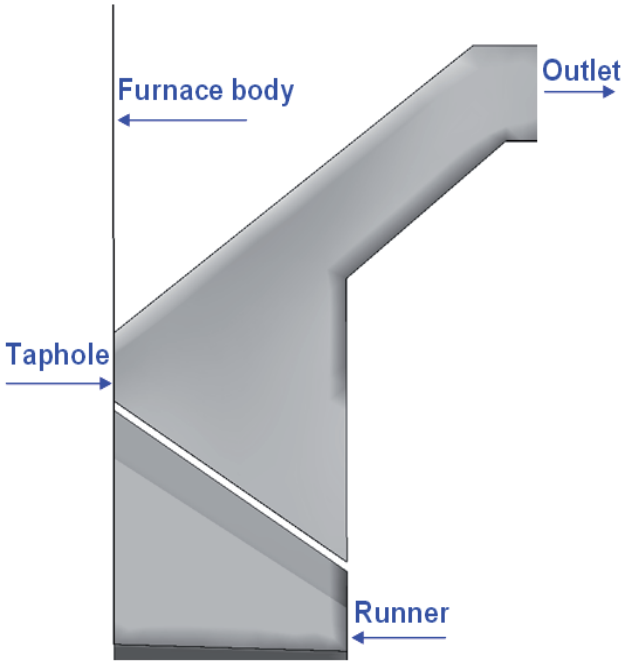

Figure 4: Side view of the structure of the new hood design

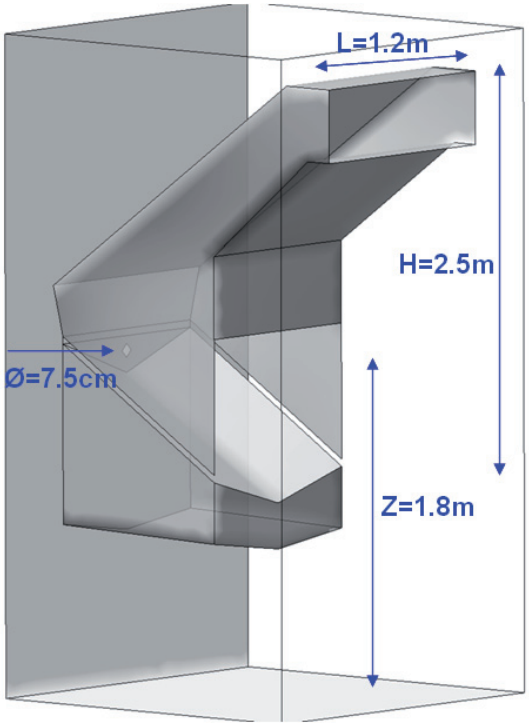

Figure 5: 3D view of the new hood design containing environment space

5 RESULTS

Totally 14 different cases based on Table 3 have been investigated in this study. Different taphole gassing modes together with different fan suctions were modeled. The results have been categorized in three different groups according to the taphole gas velocity. Although the CFD model is fully 3D but

in order to have better graphical view the central plane perpendicular to the furnace wall, and hence taphole, and parallel to the side walls of the hood has been selected to present the results.

In all these cases it was assumed that the outgoing gas from the taphole is mixture of 50% SiO and 50%CO gasses. There is no doubt that if the fraction of SiO in comparison to CO gas increases the heat generated through combustion of the off-gasses increases.

5.1 Results- Gas Velocity =10 m/s

The first case study is related to the lowest taphole gas velocity which was considered to be 10*m/s*. This case may represent a normal situation during tapping of silicon. The results of the model show that at such low velocity the gas jet is easily tilted towards the channel of the new hood design even without existence of suction created by the ventilation intake fan. Such a case is usually happens while tapping the molten silicon from the furnace but it is not the case that the new hood design has been designed for.

Contours of velocity and static temperature for the case where the suction rate is 15000 *Nm^3/hr* has been presented in Figures 6 and 7. As it can be seen from Figure 6 the gas velocity at the taphole outlet is higher than 10 *m/s* the reason is the increased kinetic energy of the gas due to high energy combustion of off-gasses. Figure 7 shows how the combustive flame has been tilted towards the channel of the new hood design. In this case the suction created by the intake fan causes some air from the furnace environment to be sucked into the channel.

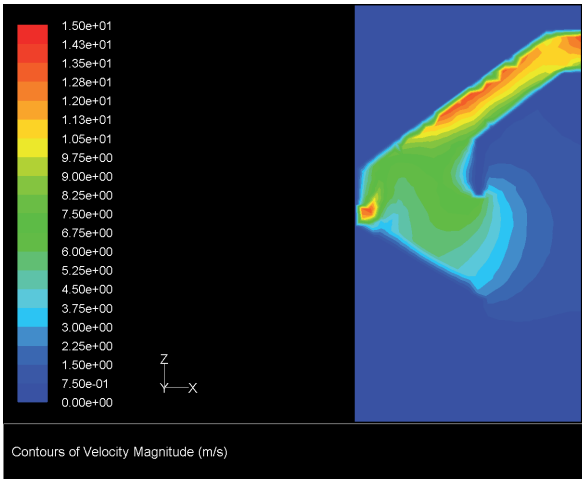

Figure 6: Contours of velocity in the central plane of the new hood channel, S=15000 *Nm^3/hr* and V=10 *m/s.*

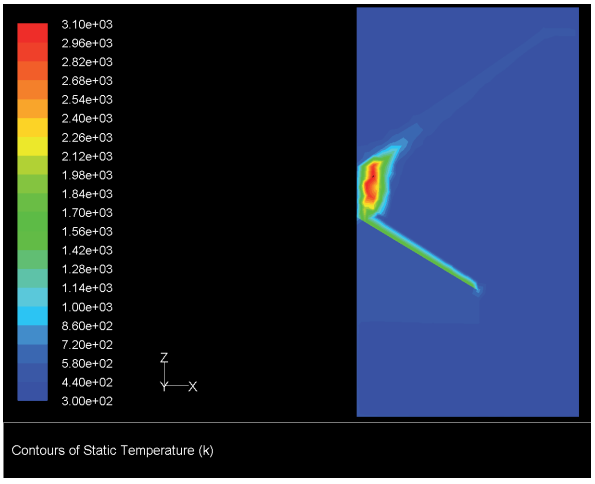

Figure 7: Ttemperature distribution in the central plane of the hood, S=15000 *Nm^3/hr* and V=10 *m/s.*

5.2 Results- Gas Velocity =50 m/s

The velocity of 50 *m/s* is the most probable value for the maximum off-gas velocity released from the taphole during taphole gassing phenomena in the real furnace operation. The results of the model show that in this case the suitable choice of suction rate created by the furnace intake fan is very important. Figure 8 shows that if the suction rate is selected to be 5000 *Nm^3/hr* some of the outgoing taphole gas can not be captured by the new hood design and will be released in the environment around the tapping area.

If the suction rate increases up to 15000 Nm^3/hr then the taphole off-gasses can be completely absorbed by the new hood design. Figure 9 represents the contours of CO_2-SiO_2 mass fraction in the previously mentioned plane in the new hood channel. In this case also some environment air is sucked into the ventilation system but it is obviously lower than the previous case. It is mainly due to higher volume of off-gasses in this case compared to the previous case study.

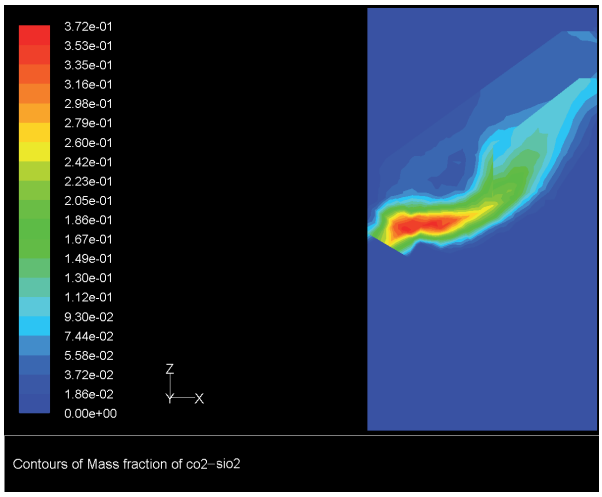

Figure 8: Contours of CO_2-SiO_2 mass fraction in the central plane of the new hood channel, S=5000 *Nm^3/hr* and V=50 *m/s.*

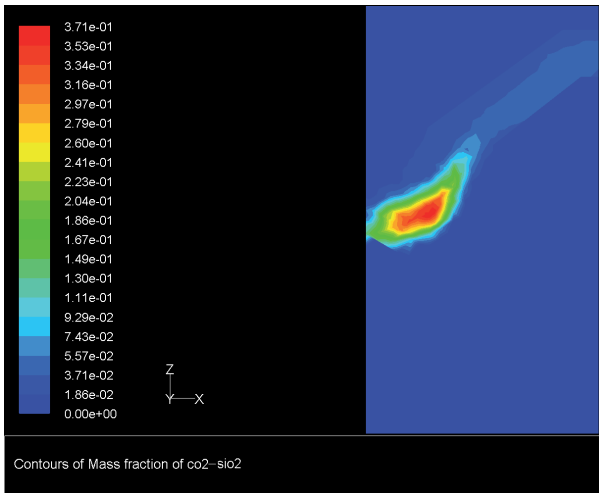

Figure 9: Contours of CO_2-SiO_2 mass fraction in the central plane of the new hood channel, S=15000 *Nm^3/hr* and V=50 *m/s.*

Figure 10 shows the temperature contours in the central plane of the new hood structure while Figure 11 represents the temperature distribution on the new hood walls and its outlet. As it can be seen from Figure 10 higher velocity of taphole off-gasses increases the combustion temperature comparing to Figure 7.

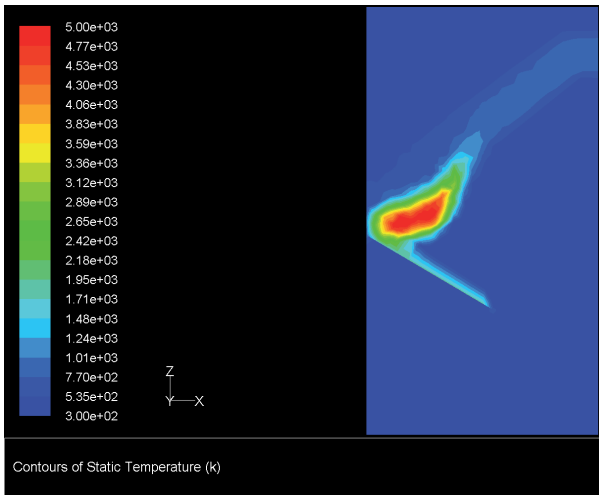

Figure 10: Ttemperature distribution in the central plane of the new hood channel, S=15000 *Nm^3/hr* and V=50 *m/s.*

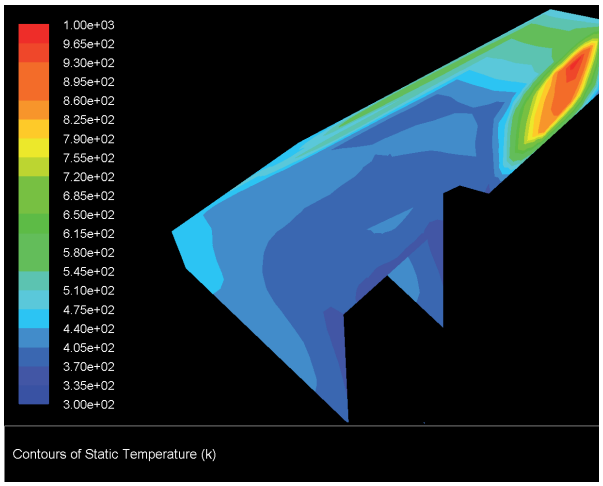

Figure 11: Ttemperature distribution on the new hood walls and its outlet, S=15000 *Nm^3/hr* and V=50 *m/s.*

5.3 Results- Gas Velocity =100 m/s

In order to show that the design of the new hood system is robust, the calculation of the model was set to the most sever case under consideration in this study the taphole gas velocity seems to be higher than what may be experienced in the normal taphole gassing phenomena. Such a gas velocity is very little probable. However the model results show that in this selection of suction rate of 30000 *Nm^3/hr* for the fan can guarantee that the total off-gasses can be absorbed by the new hood design.

Figure 12 represents the gas velocity pattern in the new hood channel. The mass fraction of the CO_2-SiO_2 gas inside the ventilation system can be seen in Figure 13.

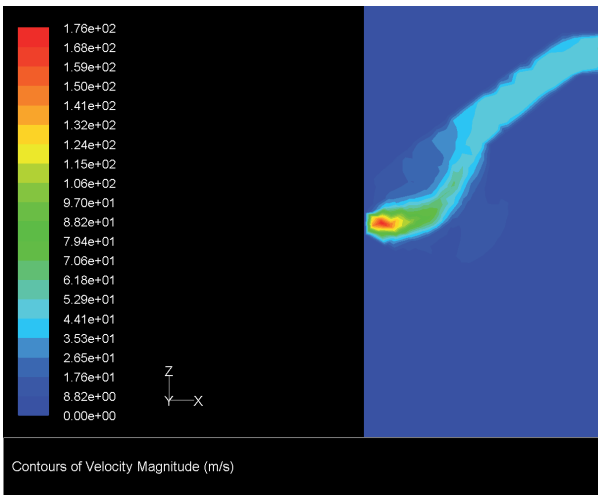

Figure 12: Contours of velocity in the central plane of the new hood channel, S=30000 *Nm^3/hr* and V=100 *m/s.*

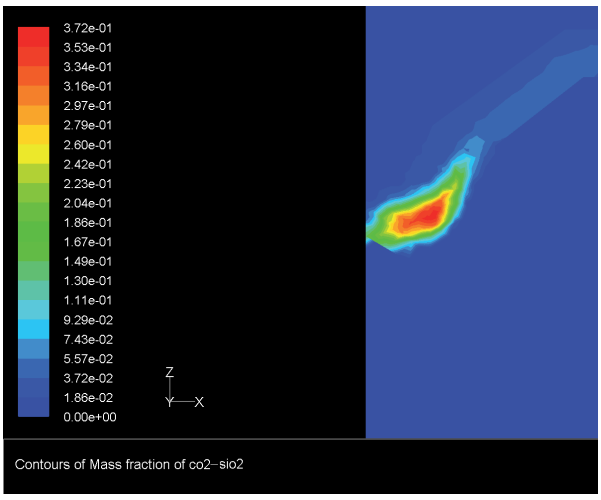

Figure 13: Contours of CO_2-SiO_2 mass fraction in the central plane of the new hood channel, S=30000 *Nm^3/hr* and V=100 *m/s.*

5.4 Results- The Effect of Taphole Gas Velocity on The Maximum Flame Temperature

The velocity of off-gasses from taphole affects the maximum temperature of the flame caused by combustion of SiO and CO gasses. The evolution of maximum flame temperature as a function of taphole gas velocity is shown in Figure 14. As it can be seen the flame temperature increases as the result of taphole gas velocity increase. But in the higher velocities its increase is very slow and it seems it is reaching to a constant value.

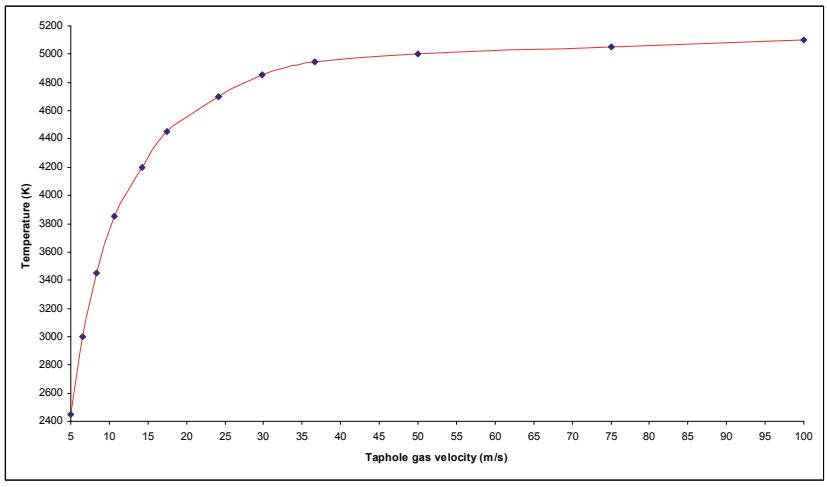

Figure 14: Evolution of maximum flame temperature with taphole gas velocity.

5.5 Validation of the Model Results

In order to validate the results of the model some tests were done at Elkem Thamshavn where the new hood design has been installed on one of the silicon producing furnaces. The results of the experiment were satisfactory and the new hood design showed very good performance in real operation.

6 CONCLUSIONS

A model for taphole gassing phenomena in silicon producing furnaces together with a new ventilation system for off-gasses released from taphole during this phenomenon has been presented. The structure of the new hood design was proposed by Elkem Company. The model is 3D and it was developed based on computational fluid dynamics (CFD) approach. The model represents different aspects of the gassing phenomena such as combustion of off-gasses, temperature distribution, different heat transfer modes, and turbulent flows off-gasses. At same time it is also able to evaluate the capabilities of the new hood design in capturing the released pollutions from the taphole. The model results for different gassing modes shows that selection of the suitable suction rate for the intake fan of the ventilation system is important in order to capture the pollutions from taphole. The total suction rate needed for the new hood design is smaller than the traditional designs. Normally the efficiency of the furnace off-gas system is affected by internal air flow around the furnace “Hall-Wind”. Due to high suction rates created by this new hood design, the efficiency of this system is less affected by “Hall-Wind”. The new hood design was installed over one of the furnaces in Elkem Thamshavn and it showed very good performance. The experimental tests in the plant are in good agreements with results generated by the model and hence it can prove the validity of the model.

7 REFERENCES

[1] Tveit, H., Halland, T., Landrø, K. I., Johansen, S. T. and Ravary, B., “The tapping process in silicon production”, Silicon for the Chemical Industry VI, 2002, 39-46.
[2] Schei, A., Tuset, J. Kr. And Tveit, H., ”Production of High Silicon Alloys”, Tapir Academic Press, Trondheim, ISBN 82-519-1317-9, 1998.
[3] Patankar, S. V.,” Numerical Heat Transfer and Fluid Flow”, Hemisphere Publishing Corporation, New York, 1980.
[4] Fluent 6.3 user’s guide ,2003, 1077-1080.
[5] Launder, B. E. and Spalding, D. B.,” Lectures in Mathematical Models of Turbulence”, Academic Press, London, England, 1972.
[6] Cheng, P.,”Two-Dimensional Radiating Gas Flow by a Moment Method”, AIAA Journal, 1964, 2:1662-1664.
[7] Siegel, R. and Howell, J. R.,”Thermal Radiation Heat Transfer”, Hemisphere Publishing Corporation, Washington DC, 1992.